Text and references accompanying Nevada Bureau of Mines and Geology Open-File Report 20-1

Geologic Map of the Petrified Spring Fault, Gabbs Valley Range, Mineral County, Nevada

by

Andrew Hoxey[1,3], Jeffrey Lee[1,4], and Andrew Calvert[2]

[1]Department of Geological Sciences, Central Washington University, Ellensburg, WA
[2]U.S. Geological Survey, Menlo Park, CA
[3]Department of Geology, University of Kansas, Lawrence, KS
[4]Department of Geophysics, Colorado School of Mines, Golden, CO

2020

Disclaimer: NBMG open-file reports have not been peer reviewed.

INTRODUCTION

Examination of 30+ year old published 1:48,000-scale geologic maps and Google Earth imagery, and field reconnaissance suggest Cenozoic volcanic-filled paleovalleys in the Gabbs Valley Range, NV (central Walker Lane) are dextrally offset by five major faults, including the Petrified Spring fault (figs. 1 and 2). New detailed geologic mapping, structural studies, and $^{40}Ar/^{39}Ar$ geochronology document offset markers across the Petrified Spring fault and form the first dataset to constrain the geometry and pre-Pleistocene slip history of the Petrified Spring fault. The Petrified Spring field area is predominantly Mesozoic metasedimentary and intrusive rocks overlain unconformably by Oligocene and Miocene tuffs and lavas offset by the Petrified Spring fault, a northwest-southeast striking, ~65 km long, dextral fault. Four Cenozoic offset markers constrain the slip history of the Petrified Spring fault. Three of these markers are volcanic-filled paleovalleys; the valley filling volcanic units yield ages of 27.24 ± 0.04 Ma (Henry and John, 2013), 15.99 ± 0.05 Ma ($^{40}Ar/^{39}Ar$ age, this study; Lee et al., in review), and 15.71 ± 0.03 Ma ($^{40}Ar/^{39}Ar$ age, this study; Lee et al, in review). The absence of measurable differential offset between the two oldest markers constrains the Petrified Spring fault's initiation age to after 15.99 ± 0.05 Ma. The two oldest markers yield an averaged dextral offset magnitude of 9.3 ± 1.5 km since ~16 Ma, indicating a minimum long-term dextral slip rate of 0.6 ± 0.1 mm/yr since the middle Miocene. The fourth marker is a line defined by the intersection of a normal fault that cuts Esmeralda Formation, which includes a volcanic ash that yields an age of 11.8 ± 0.1 Ma ($^{40}Ar/^{39}Ar$ age, this study; Lee et al. in review), and the horizontal contact between Esmeralda Formation overlying the Lavas of Mount Ferguson. The intersection line is dextrally offset 3.5 ± 1.8 km, yielding a minimum slip rate of 0.3 ± 0.2 mm/yr since ~12 Ma. These calculated long-term slip rates are equivalent, within error, to those calculated along the west adjacent dextral Benton Spring and Gumdrop Hills faults in the Gabbs Valley Range (Dubyoski et al., 2016; Mayberry and Lee, 2017; Lee et al., in review) and to GPS data constrained model estimates for current slip on the Petrified Spring fault (Bormann et al., 2016). Kinematic and structural data do not indicate a significant magnitude of vertical offset on the Petrified Spring fault.

GEOLOGIC BACKGROUND

Geologic and geodetic studies indicate the Pacific plate moves northwest at ~50 mm/yr relative the stable North American continent (e.g. Dokka and Travis, 1990; Dixon et al., 1995; Bennett et al., 2003) (fig. 1). Approximately 25% of Pacific–North American plate boundary shear is partitioned into the Walker Lane belt (WLB), a dextral shear fault system that spans a ~25–100 km wide zone across the eastern flank of the Sierra Nevada and the western boundary of the Basin and Range Province (e.g. Dokka and Travis, 1990; Dixon et al., 1995; Bennett et al., 2003; Faulds and Henry, 2008). Dextral shear is transferred through the WLB northward via the Eastern California Shear Zone, Death Valley–Fish Lake Valley fault zone, White Mountain fault zone, central Walker Lane, and northern Walker Lane (e.g. Dokka and Travis, 1990; Dixon et al., 1995; Lee et al., 2001; Stockli et al., 2003; Wesnousky, 2005; Faulds and Henry, 2008; Nagorsen-Rinke et al., 2013) (fig. 1b).

Geologic slip magnitudes and rates across the Gabbs Valley and Gillis ranges, central Walker Lane are poorly constrained because prior to this study there were no documented pre-Pleistocene offset markers across the Petrified Spring fault. Previous mapping in the Gabbs Valley metasedimentary and intrusive rocks and Cenozoic volcanic rocks (Hardyman, 1980; Ekren and Byers Jr., 1985a, 1985b,

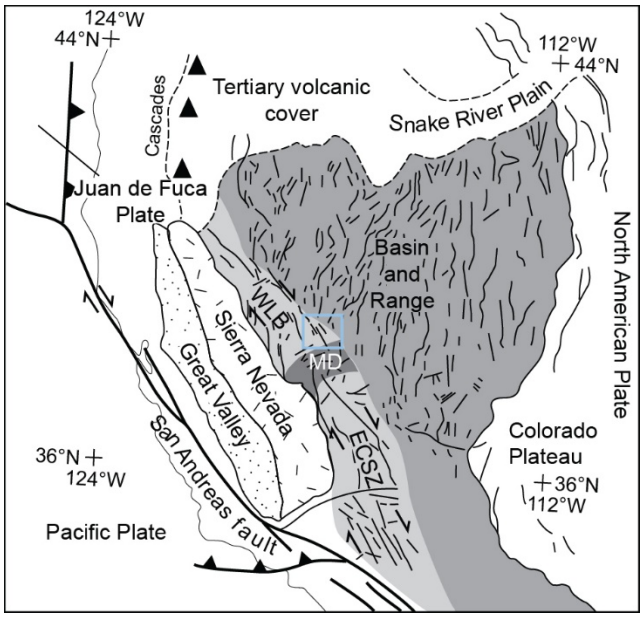

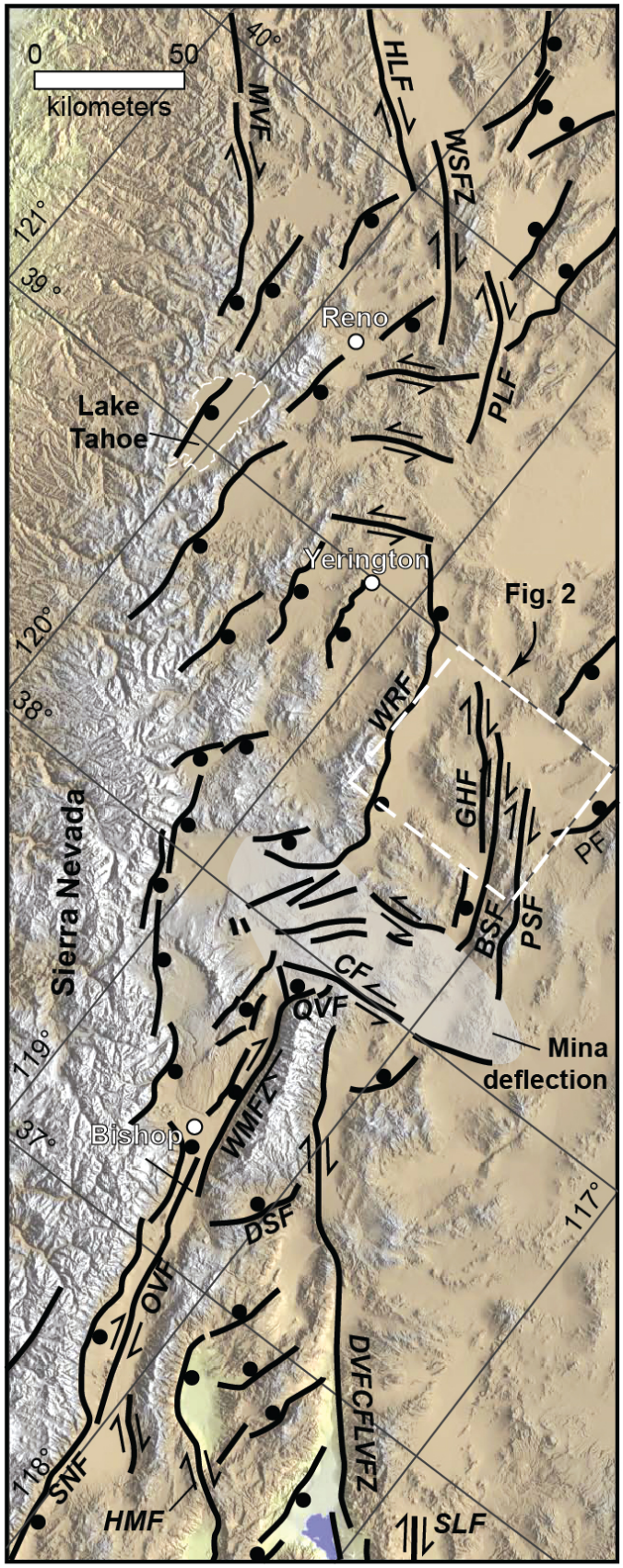

Figure 1a. (above): Simplified tectonic map of the western part of the US Cordillera showing the major geotectonic provinces and modern plate boundaries. Abbreviations: ECSZ, Eastern California Shear Zone; MD, Mina deflection; WLB, Walker Lane Belt. Blue box shows location of figure 2. Modified from Nagorsen-Rinke (2013).

Figure 1b (right): Simplified Cenozoic fault map of the Walker Lane belt. Solid ball is located on the hanging wall of normal faults; arrow pairs indicate relative motion across strike-slip faults. Fault abbreviations: BSF, Benton Spring fault; CF, Coaldale fault; DSF, Deep Springs fault; DVFCFLVFZ, Death Valley-Furnace Creek-Fish Lake Valley fault zone; GHF, Gumdrop Hills fault; HLF Honey Lake fault; HMF, Hunter Mountain fault; MVF, Mohawk Valley fault; OVF, Owens Valley fault; PF, Paradise fault; PLF, Pyramid Lake fault; PSF, Petrified Spring fault; QVF, Queen Valley fault; SLF, Stateline fault; SNF, Sierra Nevada frontal fault zone; WMFZ, White Mountains fault zone; WSFZ, Warm Springs fault zone; WRF, Wassuk Range front fault. Modified from Nagorsen-Rinke (2013).

and Gillis ranges described a succession of Mesozoic 1986a, 1986b; Oldow and Meinwald, 1992; Oldow and Dockery, 1993). The Mesozoic-Cenozoic contact geometries are highly irregular, ranging from sub-horizontal to subvertical and were interpreted as low-angle normal faults (Hardyman, 1980; Ekren and Byers Jr., 1985a, 1985b, 1986a, 1986b; Oldow and Meinwald, 1992; Oldow and Dockery, 1993). Our reconnaissance mapping in the Gabbs Valley Range suggests that the Mesozoic-Cenozoic contacts are unconformities where Cenozoic volcanic rocks are confined to approximately east-west trending paleovalleys developed within Mesozoic basement rocks. In this study, we combine geologic mapping, structural studies, and $^{40}Ar/^{39}Ar$ geochronology to document the nature of the Mesozoic-Cenozoic contact and use the volcanic-filled paleovalleys as geologic markers to document dextral offset and slip history along the Petrified Spring fault.

MESOZOIC-CENOZOIC STRATIGRAPHY

Our geologic mapping along the Petrified Spring fault documents Mesozoic basement units overlain by Oligocene, Miocene, Pliocene, and Quaternary units (sheets 1 and 2). The Mesozoic basement is comprised of intruded metasedimentary rocks overlain nonconformably by Oligocene and Miocene volcanic and sedimentary rocks. Pliocene volcanic and sedimentary rocks lie in angular unconformable contact above the Oligocene and Miocene sequence and are in turn overlain unconformably by Quaternary alluvium and colluvium deposits.

To constrain the age of volcanic units and fault history within the Petrified Spring field area, four samples were collected from Miocene volcanic and sedimentary rocks (units Mlf, Mla, Mlb, and Mles) for $^{40}Ar/^{39}Ar$ geochronology (table 1). Samples were processed following the methods described in Nagorsen-Rinke et al. (2013). Cleaned separates of sanidine, plagioclase, and groundmass were dated using incremental heating technique following the methods described in Dalrymple and Duffield (1988) and Nagorsen-Rinke et al. (2013).

Geologic Rock Units

The Mesozoic basement is comprised of the sedimentary units Triassic Luning Formation (TRlu) and the Jurassic Dunlap Formation (Jd), which were intruded by Jurassic diorite (Jdi) and a Cretaceous quartz monzonite (KJqm) (sheet 2). TRlu was mapped as undivided dolomites, limestones, and shales, which is characterized by blue and gray rounded cliffs of highly deformed limestones and dolomites. Skarn deposits within unit TRlu are regularly found at contacts with intrusive rock units Jdi and KJqm. Jd, a unit not newly described by this research, is red cross-bedded sands interbedded with shale (Ekren and Byers Jr., 1985a). Unit Jdi is characterized by dark green cliffs with parallel jointing that weathers to dark brown, and has a medium grained phaneritic texture in hand sample (Ekren and Byers Jr., 1985a). Unit KJqm is generally found cresting the highest ridges in the field area as rounded white or green cliffs. A phaneritic (plagioclase + orthoclase + quartz + biotite + hornblende + titanite) texture with conspicuous biotite phenocrysts gives KJqm a green hue in hand sample. Rounded corestones surrounded by granitic grus are locally exposed along the Cenozoic unconformity.

Lying nonconformably above the Mesozoic basement is a succession of Oligocene and Miocene volcanic and sedimentary rocks (sheet 2). At the base of the succession are the lavas of Giroux Valley (Ogslg), a pyroxene-bearing phyric basalt lava. Unit Ogslg is a ledge forming, dull-black basalt that weathers to dark rust color. Glass content increases up-section and, where exposed, the upper portion of unit Ogslg forms uniformly oriented columnar joints. Ogslg is porphyritic (plagioclase + hornblende + clinopyroxene + olivine) with hornblende ≤1.5 mm and clinopyroxene ≤2 mm.

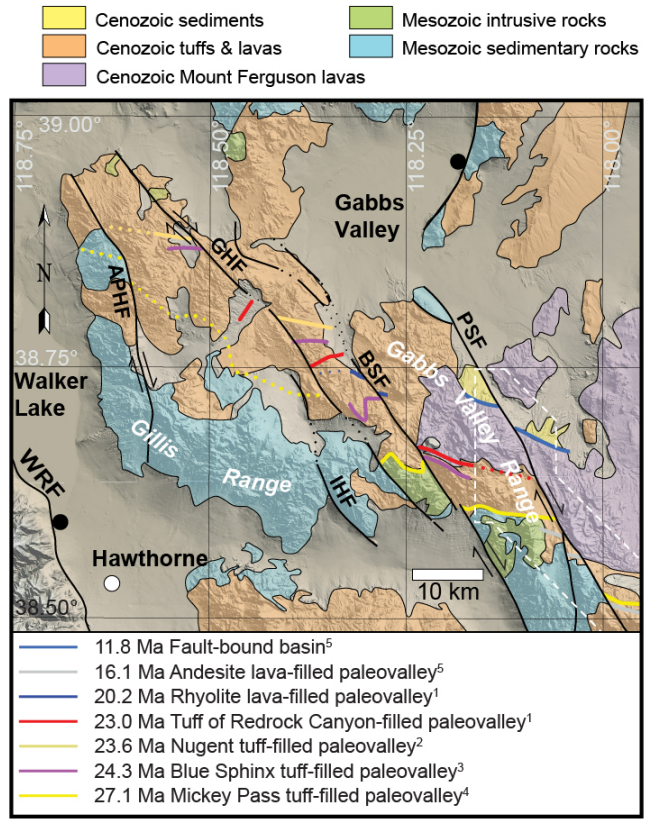

Figure 2. Shaded-relief map of the Gabbs Valley and Gillis ranges, central Walker Lane, showing the major Cenozoic faults and documented (solid lines) and postulated (dotted lines) volcanic-filled paleovalleys and other dextrally offset markers. Location of the Petrified Spring field area shown with dashed white polygon. Fault abbreviations not defined in figure 1: APHF, Agai Pah Hills fault; IHF, Indian Head fault. See figure 1b for location of map, additional fault abbreviations, and definition of fault symbols. Reported ages from Dubyoski et al., 2016 (1); Dilles and Gans, 1995 (2); Henry and John, 2013 (3) ; Henry and Faulds, 2010 (4); this study (5).

Unconformably atop unit Ogslg is the Benton Spring Group, a series of rhyolitic to dacitic tuffs with varying composition and texture. The stratigraphically lowest tuff is the Guild Mine Member of the Mickey Pass Tuff of Benton Spring Group (Ogbmg), a rhyodacite to rhyolite with multiple cooling units. The base of the unit has flow-banded vitrophyre characterized by abundant gray lithics (≤30%) and purple–dark gray flow banding. Ogbmg weathers to dark brown with weathered out fiamme pits ≤5 cm in length. Up section, unit Ogbmg forms a white flaggy yellow outcrop pattern, lacks lithics, and has abundant quartz phenocrysts. The upper section of unit Ogbmg lacks large fiamme, is porphyritic (quartz + plagioclase + biotite), and is moderately to densely welded. Embayed quartz ≤2 mm and biotite phenocrysts are found throughout, and are diagnostic for the unit (fig. 3a). Ogbmg has a reported sanidine $^{40}Ar/^{39}Ar$ age of 27.24 ± 0.04 Ma (Henry and John, 2013), a thickness of 0–300 m, and is found throughout western Nevada (e.g. Henry and John, 2013).

Table 1. New $^{40}Ar/^{39}Ar$ geochronology ages.

Unit	Sample #	Latitude	Longitude	Mineral	Age ± error (Ma)
Esmeralda volcanic ash (Mıes)	PSF17077A	38.66507	-118.07804	anorthoclase	11.8 ± 0.1
Basalt lava flow (Mıb)	PSF17052	38.52970	-117.98078	groundmass	15.71 ± 0.03
Basalt lava flow (Mıb)	PSF17045A	38.53338	-118.00771	groundmass	15.7 ± 0.2
Andesite lava (Mıal)	BS8	38.57867	-118.07466	plagioclase	15.99 ± 0.05
Lavas of Mount Ferguson (Mılf)	PSF17077B	38.66404	-118.09035	plagioclase	18.91 ± 0.03

§WMPA, weighted mean plateau age

The second unit in the Benton Spring Group is the Singatse Tuff (Ogbsi), a rhyodacite to rhyolite, multiple cooling unit with varying degrees of welding. Ogbsi has a flaggy outcrop pattern, but is generally slope forming. Most easily distinguishable by the dark red color and presence of granitic lithics (15%), this unit is porphyritic (plagioclase + quartz + orthoclase + biotite + hornblende) with plagioclase and quartz ≤2.5 mm, and biotite ≤1 mm clearly visible in hand sample. Ogbsi is densely welded in the southern section of field area with clear flow banding textured of brown-red glass and well-developed hexagonal joints. Ogbsi yields a sanidine $^{40}Ar/^{39}Ar$ age of 26.85 ± 0.02 Ma (Henry and John, 2013).

The stratigraphic top of the Benton Spring Group exposed in the Petrified Spring field area is the Petrified Spring Tuff (Ogbp). Ogbp is a biotite and plagioclase-bearing poorly welded tuff. Rich in lithic fragments (45%), the tuff has a conglomerate-like appearance at outcrop scale, and weathers to rounded gray ledges with meter-scale tafoni. Diagnostic 40 cm flattened, white pumice clasts are easily recognizable against gray matrix. Flattened cuspate shaped glass fragments are visible in thin section (plagioclase + biotite + glass). Ogbp is approximately 0–100± m thick.

Unconformably atop the Benton Spring Group is another Oligocene tuff, the Blue Sphinx Tuff (Ogsp). Ogsp is a light-gray, moderately welded quartz latite that forms ledges and easily weathers to gray rounded faces. This unit is light-purple or white on fresh faces with diagnostic white pumice ≤3 cm and conspicuous embayed quartz ≤1.5 mm surrounded by biotite-rich purple ground mass. Extensively hydrothermally altered, Ogsp is porphyritic (plagioclase + quartz + hornblende + biotite) with plagioclase phenocrysts ≤2 mm and abundant plagioclase microbreccia ≤50 μm. Sanidine $^{40}Ar/^{39}Ar$ geochronology yields an age of 24.30 ± 0.01 Ma (Henry and John, 2013).

Unconformably atop Ogsp are the lavas of Nugent Wash (Ogln). Previously published data describes unit Ogln as a hornblende-bearing andesite lava (Ekren and Byers Jr., 1985a; Mayberry and Lee, 2017). In outcrop the unit is a slope-forming, dark red-brown- to dark-gray. Plagioclase phenocryst-rich layers ≤8 mm and hornblendes 1–10 mm are diagnostic (Ekren and Byers Jr., 1985a; Mayberry and Lee, 2017).

Ogln and Ogsp are crosscut by mafic intrusions (Mımi). Mımi are basaltic-andesites that are dark brown or gray, strongly phyric (plagioclase + clinopyroxene + biotite) with a distinctive flaggy outcrop pattern (Ekren and Byers Jr., 1985a; Dubyoski et al., 2016). Plagioclase $^{40}Ar/^{39}Ar$ geochronology of unit Mımi yields an age of 23.96 ± 0.23 Ma (Dubyoski et al., 2016).

Lying unconformably above the Oligocene volcanic sequence is the Hu-pwi Rhyodacite (Mılr), a multiple cooling unit tuff and lava sequence, with one member exposed in the Petrified Spring field area. Unit Mılr is a densely welded, flow-banded, cliff-forming unit rich in black glass (30%) that weathers to light rust color. Erosion resistant, preserving sharp joint intersections on cliff faces, Mılr fractures into sharp, conchoidal glassy shards. Vitrified, flattened fiamme ≤10 cm long result in a tiger-stripe texture at outcrop scale that is diagnostic for the unit. Unit Mılr is porphyritic (plagioclase + hornblende + clinopyroxene + glass) with plagioclase phenocrysts ≤1.5 mm and lithics (10%) clearly visible in hand sample.

Unconformably atop unit Mılr and in direct unconformable contact with the Benton Spring Group is the tuff of Redrock Canyon (Mırc). In the Petrified Spring field area, unit Mırc is a rhyodacite to quartz latite, poorly welded and slope-forming with gray ash that stains orange-brown. Where moderately welded and ledge forming, there are abundant fiamme ≤10 cm in length and randomly oriented columnar joints. Lithics (10–30%) of Mesozoic granites and volcanic rocks ≤20 cm diameter are diagnostic. Mırc is phenocryst-rich (plagioclase + quartz + prehnite + biotite + hornblende) with plagioclase ≤2 mm, plagioclase microbreccia, and embayed quartz ≤2 mm. Unit Mırc has significant prehnite content, likely contributing to yellow outcrop color in the Petrified Spring field area. Sanidine $^{40}Ar/^{39}Ar$ geochronology yields an age of 22.95 ± 0.04 Ma (this study; Lee et al., in review).

Unconformably overlying Mırc and in direct unconformable contact with the tuffs of the Benton Spring Group are the Mount Ferguson sedimentary rocks (Mıs) and the lavas of Mount Ferguson (Mılf). Unit Mıs is a hornblende-bearing tuff and lahar deposit interbedded with tuffaceous fluviolacustrine deposits. The bottom of the unit is primarily fine sands and muds interbedded with tuffaceous coarse-grained sands that buttress against exposures of Mırc in the central portion of the field area. Moving up section, unit Mıs is a slope forming white and gray, lithic-rich tuff interbedded with cross-bedded tuffaceous sediments. The tuff is interbedded and overlain by debris flows primarily composed of Mount Ferguson volcanic rocks with boulders ≤1.5 m diameter and petrified logs ≤2 m in length and 0.5 m in diameter. Mılf conformably overlies and is interbedded with Mıs. Mılf is comprised of undivided lavas; hornblende-bearing andesitic, phenocryst-rich (plagioclase + hornblende + pyroxene) flows of varying composition and texture,

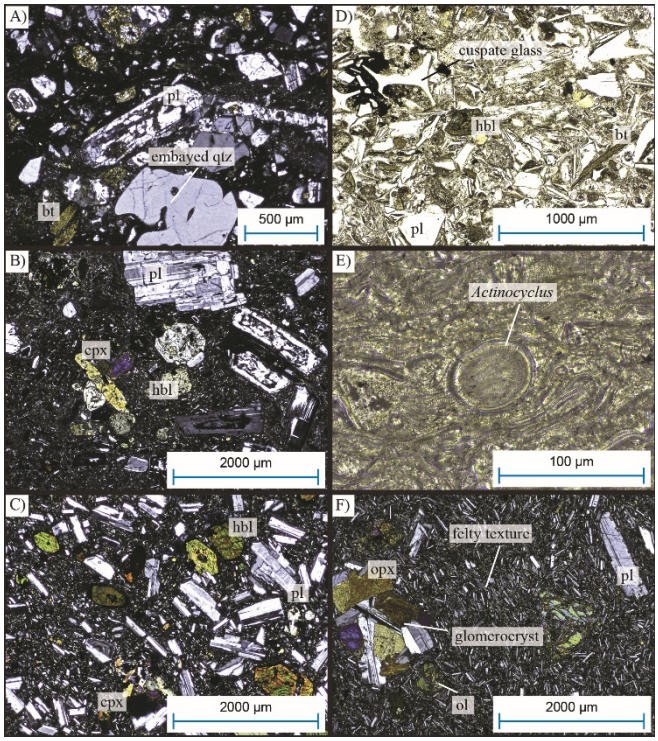

Figure 3. Annotated photomicrographs of several Cenozoic units. (A) Guild Mine Member of Mickey Pass Tuff (unit Ꝏbmg). (B) Lavas of Mount Ferguson (unit Mɪlf). (C) Andesite lava (unit Mɪal). (D) Esmeralda sands (unit Mɪs). (E) Esmeralda Formation (unit Mɪe). Thin section cut perpendicular to bedding. (F) Basalt lava flow (unit Mɪb). All photomicrographs in cross-polarized light, except D and E in plane-polarized light. Mineral abbreviations: bt, biotite; cpx, clinopyroxene; hbl, hornblende; pl, plagiocalse; ol, olivine; qtz, quartz.

ranging from light-gray hornblende-rich to dark-red with plagioclase phenocrysts ≤3 mm (fig. 3b). Mɪlf is mostly dark, ledge-forming flows with columnar jointing that lacks consistent orientation. In phenocryst-rich samples, a dark-red and black banding texture is diagnostic. Plagioclase from a lava flow near the top of unit Mɪlf yields an $^{40}Ar/^{39}Ar$ age of 18.91 ± 0.03 Ma (this study; Lee et al., in review).

Interfingering within Mɪlf in the Petrified Spring field area and crosscutting as a dome structure in other localities within the Gabbs Valley Range is the rhyolite of Gabbs Valley Range (Mɪrl) (Ekren and Byers Jr., 1985a). Unit Mɪrl is a flow-laminated biotite-bearing rhyolite that outcrops as white- to light-purple rounded cliffs with well-developed foliation. Devitrified glassy groundmass leads to highly friable material that weathers to granular white soil. Mɪrl is porphyritic (plagioclase + quartz + biotite + hornblende) with conspicuous biotite flakes ≤1 mm in a white matrix diagnostic in hand sample. Embayed quartz grains ≤1 mm are visible in thin section. Plagioclase $^{40}Ar/^{39}Ar$ geochronology yields an age of 20.14 ± 0.26 Ma (this study; Lee et al, in review).

Unconformably above unit Mɪlf lies a Miocene alluvium and colluvium sedimentary unit (Mɪac). Highly variable in thickness, Mɪac is comprised of rounded cobbles of dominantly Oligocene volcanic rocks and lesser Mesozoic units. Unit Mɪac outcrops as slopes of unconsolidated rounded clasts of gravel to cobbles ≤20 cm in diameter that commonly weather to light rust color, giving the map extent a red hue in aerial photos. Clast lithologies include granite, limestone, mudstone, vesiculated rhyolite lava, and quartz-rich welded tuff. Quartz-rich volcanic rocks are presumed to be remobilized Benton Spring Group volcanic rocks, other volcanic clasts are likely sourced from Mɪlf. Unit Mɪac is regularly found in direct depositional contact with the Mesozoic basement. As a result, the age of unit Mɪac is not well constrained. However, given the clast source, unit Mɪac likely fills a basin that developed adjacent to Mount Ferguson after emplacement of unit Mɪlf.

Conformably atop unit Mɪac is a hornblende-bearing andesite tuff (Mɪat). Mɪat is a poorly exposed, slope-forming, lithic-rich tuff with a poorly welded white ash matrix. Light-gray to white where fresh, the unit weathers to white granulated soil. Lithic fragments (30%) in the tuff include local Mesozoic rocks and hornblende-bearing volcanic rocks. Unit Mɪat has pumice clasts ≤30 cm in diameter with euhedral plagioclase ≤1.5 mm and hornblendes ≤2 mm with oxy-hornblende rims (plagioclase + hornblende + clinopyroxene).

Conformably overlying unit Mɪac and interbedded with unit Mɪat is a hornblende-bearing andesite lava (Mɪal). Presumed to be genetically related to Mɪat, Mɪal is ledge forming, blue-gray or dark gray-black, and weathers to a dark rust color. There are three distinguishable sections, presumed to be separate flows; the base is characterized by well-developed columnar jointing and platy jointing; the middle of the unit is gray and foliated, with an aligned hornblende lineation; and the upper section is dark brown and relatively phenocryst-poor with randomly oriented cooling joints. Mɪal is porphyritic (plagioclase + hornblende + clinopyroxene) with conspicuous needle-shaped 1–2 mm hornblende phenocrysts with thick oxy-hornblende rims (fig. 3c). Plagioclase $^{40}Ar/^{39}Ar$ geochronology yields an age of 15.99 ± 0.05 Ma (this study; Lee et al., in review).

Unconformably overlying the Oligocene and Miocene volcanic succession are basin-filling sediments of the Esmeralda Formation (Mɪes and Mɪe). The Esmeralda sands member of the Esmeralda Formation (Mɪes) are massive deposits of sands and volcanic ash that weather to smooth white ledges with 0.5–2 m tafoni. Unit Mɪes, a lithic graywacke, is composed of rounded volcanic clasts ≤15 cm suspended in a matrix of sands and muds rich in lithic minerals. Mɪes is interbedded with crystal-rich, very fine, white ash material with cuspate glass shards visible in thin section (fig. 3d). $^{40}Ar/^{39}Ar$ geochronology of anorthoclase from an ash bed in unit Mɪes yields a laser fusion age of 11.8 ± 0.1 Ma (this study). Esmeralda Formation undivided (Mɪe) is composed of thin (10–15 cm) bedded white silts and muds that weather to a highly friable, papery texture. Occasional medium to course sand are densely compacted with 3-D current ripples and flame structures. In thin section papery silt layers are observed as stacked ~50 µm diameter Actinocyclus diatoms, suggesting a middle Miocene age (Krebs et al., 1987) (fig. 3e). Beds are strongly deformed near fault contacts.

A Miocene basalt lava flow (Mlb) interfingers with the Esmeralda Formation in the southern portion of the field area. Mlb is a ledge-forming black basalt that weathers to dark rust color with poorly developed columns ~1 m wide and platy jointing spaced ~5 cm. Phenocryst-bearing (plagioclase + orthopyroxene + olivine), this basalt lava has subhorizontal veins found at the base of the unit filled with quartz geodes. In thin section, microcrystalline plagioclase has felty texture and glomerocrysts of plagioclase and pyroxenes 0.5–1.5 mm are visible (fig. 3f). Groundmass $^{40}Ar/^{39}Ar$ geochronology yields an age of 15.71 ± 0.03 Ma (this study; Lee et al., in review).

Crosscutting the Miocene sediments in the southern portion of the field area is a weakly phyric plagioclase-bearing diorite (PzMlmi). Unit PzMlmi is a black mafic intrusion that weathers to light rust color and erodes to a yellow-brown granulated soil. PzMlmi is a phyric (plagioclase + hornblende + oxides) plagioclase-bearing diorite with ≤1 mm domains of uralite alteration visible in thin section. Microcrystalline plagioclase shows felty texture and elongate mineral alignment in thin section. The relative age relationship of unit PzMlmi is poorly constrained given lack of contact exposure, but PzMlmi is presumed intrusive given phenocryst texture and percentage (100%).

Two basalt flows of unknown absolute age were identified in the field area, both of which lie unconformably above unit Mle, but are not in close proximity to each other. The first basalt lava flow (PzMlb$_1$) is phyric (plagioclase + orthopyroxene + olivine) and a ledge-forming, columnar jointed basalt that is dark gray where fresh and black to dark rust where weathered. PzMlb$_1$ is differentiable from units Mlb and PzMlb$_2$ by its abundant >1 mm plagioclase phenocrysts, surrounded by black and red banded ground mass. Basalt lava flow 2 (PzMlb$_2$) forms an extensive plateau at the southern end of the field area, Table Mountain, and sits unconformably atop the Mesozoic basement rocks (sheet 1). Unit PzMlb$_2$ is a ledge former with 1–2 m hexagonal jointing that lacks consistent orientation. In hand sample PzMlb$_2$ is markedly aphanitic with flattened vesicles. In thin section microcrystalline, zoned plagioclase are visible (plagioclase + glass + oxides).

Two inactive Quaternary deposits were documented lying unconformably atop the Oligocene, Miocene, and Pliocene volcanic and sedimentary succession. A fanglomerate (QPzfg) is comprised of consolidated material, poorly bedded and poorly sorted clasts of presumed local origin. Clasts are rounded to subrounded gravel to cobble sized. Distinguishable from unit QPzf by degree of consolidation. Distinguishable from Mac by high percentage of Mesozoic intrusive rocks (~20%) and small percentage of Benton Spring Group volcanic rocks (<10%); remaining clasts are sourced from units Tlu, Mlf, and Mlal. The unit is presumed Quaternary-Pliocene in age given the abundance of underlying volcanic rocks. The second inactive Quaternary deposit (QPzf) is clay to gravel-sized unconsolidated sediment topographically high relative to active fans, forming ridge and ravine topography. QPzf is composed of subrounded clasts of various volcanic rocks ranging in size from pebbles to ~30 cm boulders. Clast composition is highly variable with well-developed desert varnish and ventifacts.

Other Quaternary mapped units include active alluvial-fans (Qf), landslide deposits (Qls), and, seasonally active streams (Qal). Qf is recognized by clay to gravel-sized unconsolidated fluvial sediment with subangular cobbles and pebbles. Unit Qf surfaces have moderate-well developed desert pavement with occasional well developed ventifacts. Unit Qls is characterized by alluvium, and colluvium surrounding intact slumped blocks of local units. Unit Qls has a diagnostic hummocky topography with several randomly oriented ~50 m^2 blocks of presumed locally derived remobilized rocks. Qal is comprised of alluvium in seasonally active stream beds and channels. Qal is identifiable by unconsolidated medium-course grained sands and gravels. The map unit includes vegetated flats between ranges.

Our map also includes anthropogenic deposits (Htp) of waste material associated with local open-pit mining.

Paleovalleys

We observed corestones, grus, paleosols, and gravels at the Mesozoic-Cenozoic contacts in the Petrified Spring field area, leading us to an interpretation of unconformities that define the base of sublinear paleovalleys incised into Mesozoic basement and filled with Cenozoic volcanic rocks. This interpretation is in contrast to low angle normal fault contact between Mesozoic basement and Cenozoic volcanic rocks shown in the 1:48,000-scale geologic maps published in the 1980s (Ekren et al., 1980; Ekren and Byers Jr., 1985a). We identified three, approximately east-west trending, 2–4 km wide, gravel and paleosol floored paleovalleys that restricted flow of volcanic material, preserving linear map traces that were truncated by subsequent faulting (sheet 1).

The oldest paleovalley mapped in the Petrified Spring field area is a series of nested east-west trending, approximately 4–6 km wide, lava- and tuff-filled paleovalleys incised into Mesozoic metasedimentary and intrusive rocks (sheet 1; cross section C–C' on sheet 2). Unit Ogslg (defining an ~2 km wide, ≥50 m thick paleovalley) infilled the incised Mesozoic units and was subsequently Ogsbp, which comprise the Benton Spring Group (defining an ~4 km wide, ~1000 m thick paleovalley). The Benton Spring Group tuffs were then incised before emplacement of unit Ogssp (defining a ~1 km wide, ~50 m thick paleovalley), which was subsequently incised before emplacement of incised before emplacement of units Ogsbmg, Ogsbsi, and units Ogsln and Mlrc (defining a ~1 km wide, ~300 m thick paleovalley). The repeated incision and emplacement results in the nested geometry has been observed elsewhere in the Great Basin (e.g. Colgan and Henry, 2017). The nested geometry suggests a long-standing (millions of years) drainage network, leading to significant lateral variation in unit thickness, and resulting in non-linear map patterns of some paleovalley filling units.

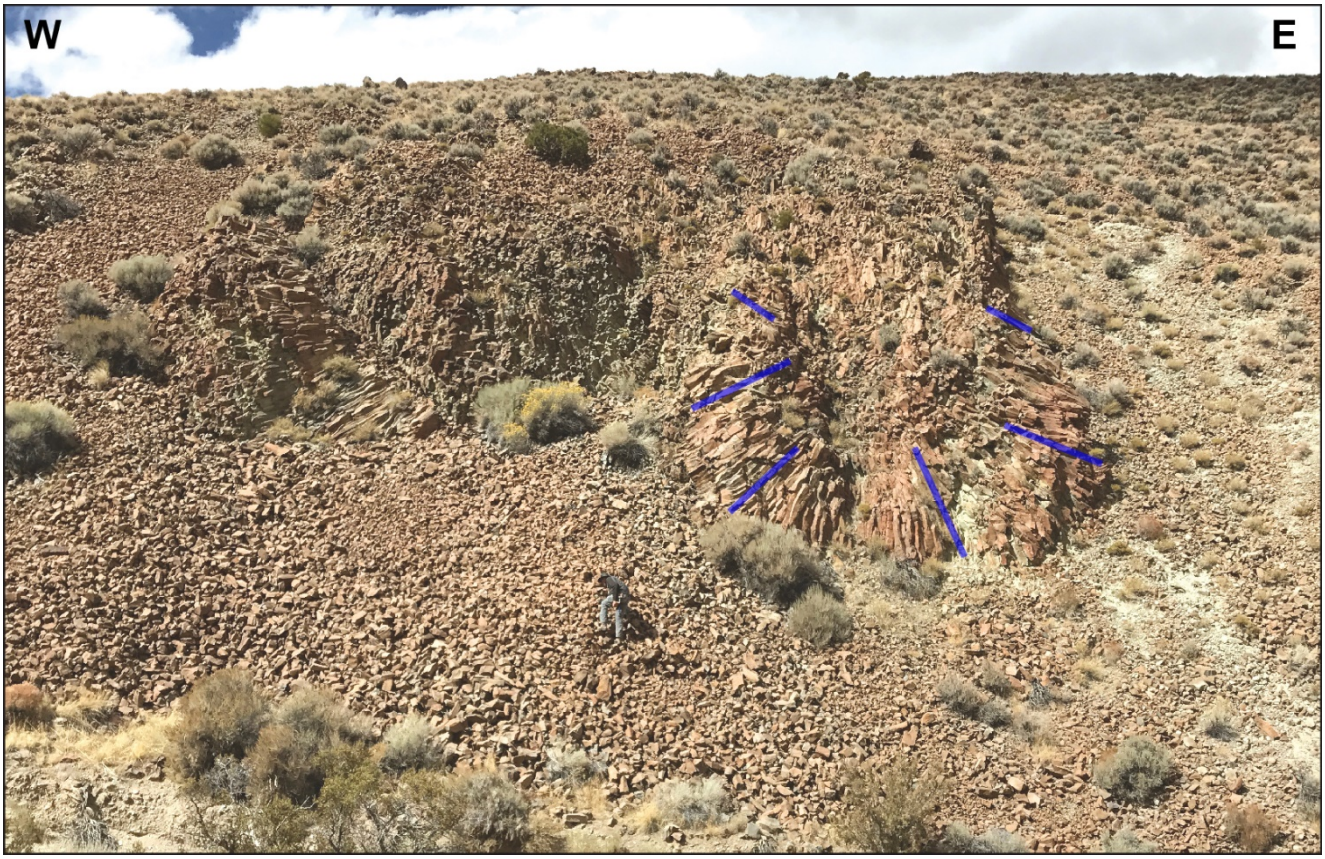

Figure 4. Field photograph of columnar rosette in unit Mrat. Blue lines mimic orientation of ~5–10 cm diameter columns. Geologist in the center for scale.

The southern boundary of the nested paleovalley series filled with Benton Spring Group tuffs is well defined by an east-west striking normal fault in the Mesozoic rocks (sheet 1). We observed compaction foliations in unit Ogbmg at the base of the nested paleovalley series. A parallel relationship between compaction foliations and contact orientations, which would strongly suggest compaction against a paleotopographic surface, was not observed (Henry and Faulds, 2010). Observation of closely spaced variation in orientation of the compaction foliation suggests turbulence in the flowing tuff during emplacement and welding caused by close proximity to irregularities in paleotopography; a strong indicator this is the basal section of the flow (Henry and Faulds, 2010). Lack of breccia or fault gouge in the Cenozoic volcanic rock suggests the east-west trending normal fault has been inactive since tuff emplacement. We propose that the normal fault's footwall side was exposed at the surface during tuff emplacement, and that the east-west trending escarpment formed the southern valley wall (sheet 1; cross section C–C' on sheet 2). The northern paleovalley wall is obscured by the overlying younger Mrlf.

The second, younger paleovalley, also incised into Mesozoic rocks, and filled with units Mrac and Mral (sheet 1; cross section D–D' on sheet 2). The contact between units KJqm and Mrac is characterized by ≤2 m thick grus deposits surrounding ≤1.5 m spheroidal weathered corestones, suggesting a period of subaerial exposure. At the northern extent of the paleovalley, the contact is subhorizontal with broad (~100 m length, ~10 m height) undulation and is commonly found partially filled with unit Mrac. The abundance of rounded and subrounded clasts and lack of angular clasts, suggests that unit Mrac is a gravel deposit within an east-west trending fluvial paleovalley that broadens (~2–4 km) from east to west, an interpretation in contrast to Ekren and Byers Jr. (1985a) conclusion that unit Mrac was a remnant alluvial-fan deposit. In the deepest segments of this paleovalley, we observe ≤100 m thick deposits of unit Mrat, a hornblende-bearing tuff. In a densely welded portion of unit Mrat, columnar joints form an ~15 m wide rosette pattern (fig. 4), likely the result of evacuation of superheated fluids during tuff emplacement over an active fluvial environment (Wright et al., 2011).

Where unit Mral is observed in direct contact with the Mesozoic basement it is commonly found in near-vertical contact, suggesting topography was characterized by a steep-sided canyon partially filled with gravels of unit Mrac during emplacement of unit Mral (sheet 1; cross section D–D' on sheet 2). In contrast, at the southernmost exposures of Mral against Mesozoic rocks, the contact is subhorizontal and the basal, platy jointed, sections of unit Mral are not present. We interpret the near vertical contact as a paleovalley wall in a narrow (~1 km) portion of the paleovalley and the southernmost exposures as evidence that unit Mral filled the paleovalley before overflowing onto an adjacent floodplain.

The youngest paleovalley identified in the Petrified Spring field area is incised into lacustrine sediments, unit Mre, and filled with a basalt lava flow, unit Mrb (sheet 1; cross section E–E' on sheet 2). The contact shows an arcuate, concave-up geometry with radial columnar joints in the overlying Mrb. A pole to the best-fit circle of measured columnar joints yields a 63° axis trend of the arcuate contact. We interpret the radial distribution of the columnar joints as indicative of a paleovalley here trending northeast-southwest.

STRUCTURAL GEOLOGY

The Petrified Spring fault is a NW-SE striking, near vertical dextral fault that is a single, through-going fault in the north end of the field area, and splits into several splays in the south where it connects with the dextral Bettles Well fault (Oldow and Meinwald, 1992) (sheet 1). In the northern section of the field area, the fault's surface expression is characterized by offset channels and alluvial-fan surfaces. Fault scarps, shutter ridges, and offset channels consistently show dextral displacement. Fault exposure in pre-Pleistocene aged rocks is rare. However, along the contact with unit Mrlf, we observed a ~4 cm wide zone of gouge and a fault plane with an average strike of 332° and a dip of 87° northeast.

Extending south from this region, the Petrified Spring fault trifurcates and offsets a deeply incised channel, then appears to merge into a single trace defining the eastern flank of Calavada Flat in the central portion of the field area (sheet 1). Here, a steep west-facing cliff-face of unit Mrlf dominates the topography (sheet 1). Given the fault's character south of Calavada Flat, it is possible that multiple fault splays are buried by the Quaternary sediments in the flat, but the steep cliff and adjacent shutter ridges are the best evidence for the map trace of the fault.

In the southern portion of the field area, the fault splays into multiple strands which are recognized by linear lithologic contacts that crosscut topography. Exposure of the fault plane is rare, though lithologic contact geometries and occasional travertine deposits act as strong indicators for the map pattern of the fault. In one location, a ~2 m zone of brecciated Mesozoic metasedimentary rocks, unit TRlu, is exposed with an averaged strike of 329° and dip of 70° northeast. Offset fan deposits, unit QPbf, and strongly folded and upturned Miocene lacustrine sediments, unit Mre, also serve as evidence for fault motion.

Dextral and Vertical Slip

New geologic mapping in the Petrified Spring field area documents four Cenozoic geologic markers dextrally offset by the Petrified Spring fault (sheet 1, dextrally offset markers 1–4; table 2): (1) a set of Oligocene nested paleovalleys, (2) a Miocene paleovalley incised in Mesozoic basement, (3) a Miocene paleovalley incised in Miocene sediments, and (4) a Miocene basin-bounding normal fault. Offset measurements were made using the 1:24,000-scale geologic map in sheet 1 digitally overlain on Google Earth imagery, projecting markers into the trace of the Petrified Spring fault as needed, and measuring parallel to the map trace of the Petrified Spring fault with Google Earth line segments.

The first and oldest marker is a series of nested paleovalleys defined by a sublinear, subvertical nonconformable contact between Oligocene volcanic rocks, the Benton Spring Group tuffs, to the north deposited against Mesozoic metasediments and intrusive rocks to the south. The paleovalley filled with units OGlg, OGbmg, and OGbsi is truncated into three fault blocks and dextrally offset by the Petrified Spring fault. On the west side of the Petrified Spring fault, the southern boundary of the nested paleovalley is well defined by a near vertical contact (sheet 1, offset marker 1–1'). On the east side of the Petrified Spring fault, the contact is buried by a Quaternary landslide. The location is, thus, estimated and projected to within 2.5 km and 0.5 km on the west and east sides of the Petrified Spring fault, respectively, yielding a squared sum of ± 2.5 km of error associated with our offset measurement. The measured dextral offset of the Benton Spring Group nested paleovalley is 10.3 ± 2.5 km across the Petrified Spring fault. Dividing the 10.3 ± 2.5 km dextral offset by the reported sanidine $^{40}Ar/^{39}Ar$ age of 27.24 ± 0.04 Ma (Henry and John, 2013) for the youngest, most clearly exposed unit in the nested series, OGbmg, yields a long-term, minimum dextral slip rate of 0.4 ± 0.1 mm/yr across the Petrified Spring fault since the middle Oligocene. Offset magnitudes for the second and next-youngest geologic marker, the paleovalley filled with unit Mral, are similarly projected and estimated (sheet 1, offset marker 2–2'). Unit Mral is truncated into four fault blocks and dextrally offset by the Petrified Spring fault (*i–iv* on sheet 1). The paleovalley width in block (*i*), at ~2.2 km, is inferred to match well exposed north-south width of unit Mral in block (*ii*). The southern contact is thus inferred as an

Table 2. Calculated dextral slip rates along the Petrified Spring fault.

Offset marker, number§	Age ± error (Ma)	Age source	Dextral offset (km)
Guild Mine Member of the Mickey Pass Tuff (OGbmg), 1	27.24 ± 0.04	Henry & John (2013)	10.3 ± 2.5
Andesite lava (Mral), 2	15.99 ± 0.05	this study	8.2 ± 2.3
Basalt lava flow (Mrb), 3	15.71 ± 0.03	this study	>1.9 ± 0.4
Normal fault bounding Esmeralda sands (Mres), 4	11.8 ± 0.1	this study	3.5 ± 1.3

§number is tied to marker shown on sheet 1.
***dextral offset measurable across only two of the three fault splays.**

eroded, near-vertical contact at the southern end of block (*i*), through present-day Sunrise Flat, inferring a broadening of the paleovalley co-located with a deposits of unit Mrac. At the southern extent of unit Mral in block (*ii*), unit Mral buttresses against Mesozoic basement rocks as a near vertical contact. The contact is directly truncated by the west-most fault splay, negating the need for a projection. The measured dextral offset across the westernmost fault splay between blocks (*i* and *ii*) is 1.9 ± 1.0 km. Blocks (*ii* and *iii*) both have well-preserved, subvertical contacts between units Mral and Ꞧlu, interpreted as steep paleovalley walls in a relatively narrow (~1–2 km) canyon. In block (*iv*) the steep north-dipping contact is inferred through a present-day canyon. The cumulative dextral offset across blocks (*ii–iv*) is estimated to 6.3 ± 1.3 km. Summing the offset magnitudes across the three splays yields a total estimated dextral offset magnitude of 8.0 ± 2.1 km. Dividing the 8.0 ± 2.1 km offset magnitude by the plagioclase $^{40}Ar/^{39}Ar$ geochronology age of 15.99 ± 0.05 Ma for unit Mral yields a minimum long-term dextral slip rate of 0.5 ± 0.1 mm/yr across the Petrified Spring fault since the middle Miocene.

The third, and next-youngest offset marker documented in this study is a paleovalley filled with unit Mrb (sheet 1, offset marker 3–3'). Mrb outcrops on both sides of two out of three fault splays in the southern portion of the field area. The contact between unit Mrb and the underlying unit Mre defines a concave up morphology. Structural measurements from columnar joints in Mrb perpendicular to the basal contact define a best-fit great circle with a pole trending 63°, which we interpret as the longitudinal axis of a paleovalley into which Mrb flowed. Given there are no exposures of sub-vertical contacts associated with this paleovalley, the projection of the inferred paleovalley axis, assumed to be linear, is the most reliable feature for measuring offset magnitude. Using the 63° trend, unit Mrb projects into the intersection with the fault splays to within 0.25 km and 0.3 km on the west and east sides of the splays respectively, yielding a squared sum of error ± 0.4 km. The estimated 1.9 ± 0.4 km magnitude of dextral offset across the fault splays is a minimum because unit Mrb is only exposed across two of the three fault splays in the southern portion of the map area. Dividing the 1.9 ± 0.4 km offset magnitude by the groundmass $^{40}Ar/^{39}Ar$ geochronology age of 15.71 ± 0.03 Ma for unit Mrb yields a minimum long-term dextral slip rate across the two east-most fault splays of ~0.1 mm/yr since the middle Miocene.

The fourth, and youngest geologic marker is a basin-bounding normal fault truncated and dextrally offset across the Petrified Spring fault (sheet 1, offset marker 4–4'). We observed a sharp change in topography associated with the northern map extent of unit Mrlf adjacent to younger sedimentary units Mres and QPof, and joints with a strike of 300° and a dip of 63° northeast, suggesting a poorly exposed normal fault. On the hanging-wall side of the fault we observe paleosol developed stratigraphically on top of the down-dropped unit Mrlf, overlain by unit Mres. The nonconformable contact of unit Mres overlying unit Mrlf in the hanging wall is indicative of a fault-bound basin that is filled with Miocene sediments, units Mres and Mre. The depositional ages of units Mres and Mre, in turn, act as an approximate constraint on the timing of slip of the normal fault. Error associated with the offset magnitude for the normal fault bound of unit Mres is attributed to both the estimated projection into the Petrified Spring fault map trace and the non-vertical nature of the normal fault contact. Based on observations discussed later in this section, the Petrified Spring fault is interpreted to have no measurable vertical offset. Furthermore, the depositional contact between the hanging-wall unit Mrlf and overlying unit Mres is observed on the east side and inferred on the west side of the Petrified Spring fault. This depositional contact, thus, produces an intersection lineation with the non-vertical fault plane. The intersection lineation acts as reliable marker that can be projected in three dimensions into the Petrified Spring fault. The intersection lineation is projected beneath Quaternary cover into the Petrified Spring fault and estimated to within 0.25 km and 1.25 km on the west and east sides respectively, yielding a squared sum error of ± 1.8 km. Projecting the intersection lineation, a dextral slip magnitude of 3.5 ± 1.8 km across the Petrified Spring fault is estimated. Dividing the 3.5 ± 1.3 km offset magnitude by the anorthoclase $^{40}Ar/^{39}Ar$ age 11.8 ± 0.1 Ma for a volcanic ash in unit Mres (this study) yields a minimum long-term dextral slip rate of 0.3 ± 0.2 mm/yr since ~12 Ma.

Our observations do not indicate a significant magnitude of vertical offset on the Petrified Spring fault (sheet 1). Field observations including alternating fault-scarp face directions, nearly vertical fault planes, and linear fault traces across topography suggest nearly pure strike-slip motion. One exposure of slickenlines, measured on a fault splay north of Calavada Flat, record a plunge of 6° towards the southeast, also indicating dominantly strike-slip motion. Given the lack of well-defined vertical offset markers, we could not document the magnitude of vertical offset, even if significant.

GEOLOGIC UNITS

Anthropogenic Deposits

Htp Tailings pile (Holocene) Topographically flat-topped pile of waste material associated with local open-pit mining. *Distinguishing features: unconsolidated angular clasts in rectangular pile.*

Recently Active Alluvial, Fluvial, And Colluvial Deposits

Qal Alluvium (Holocene to Pleistocene) Seasonally active stream beds and channels. Unconsolidated medium to course-grained sands and gravels. Includes vegetated flats between ranges. Thickness ≤50 m. *Distinguishing features: unconsolidated sand and soils.*

Qls Landslide deposits (Holocene to Pleistocene) Alluvium and colluvium surrounding intact slumped blocks of local units. Hummocky topography with several

randomly oriented ~50 m blocks of presumed locally derived remobilized volcanic rocks. Poor scarp preservation. Thickness ≤60 m. *Distinguishing features: hummocky blocks in varying orientations.*

Qf Alluvial-fan deposits (Holocene to Pleistocene) Active alluvial-fan deposits of clay to gravel-sized unconsolidated fluvial sediment. Subangular cobbles and pebbles in unconsolidated sandy matrix. Moderate to well-developed desert pavement with occasional well-developed ventifacts. Thickness ≤40 m. *Distinguishing features: gently sloped locally sourced angular sediment.*

Remnant Alluvial-fan Deposits

QPlf Older alluvial-fan deposits (Pleistocene to Pliocene) Clay to gravel-sized unconsolidated sediment topographically high relative to Qf, forming ridge and ravine topography. Subrounded clasts of volcanic rocks ranging in size from pebbles to ~30 cm boulders. Clasts are variety of lithologies, including Miocene volcanic rocks. Well-developed desert varnish with ventifacts. Thickness ≤15 m. *Distinguishing features: ridge and ravine topography with wide variety of lithologies.*

QPlfg Fanglomerate (Pleistocene to Pliocene) Consolidated remnant alluvial-fan, well-consolidated locally derived conglomerate material. Poorly bedded and poorly sorted clasts of presumed local origin. Clasts are rounded to subrounded gravel to cobble sized. Distinguishable from unit QPlf by degree of material consolidation. Distinguishable from Mac by high percentage of Mesozoic intrusive clasts (~20%) and low percentage of Benton Spring Group volcanic rocks (<10%); remaining clasts are units Ꞧlu, Mlf, and Mlal. Thickness ≤100 m. *Distinguishing features: well consolidated beds of poorly sorted sediment.*

Pliocene-Miocene Volcanic and Intrusive Rocks

PlMlmi Mafic intrusive rocks (Pliocene to Miocene) A weakly phyric plagioclase bearing diorite. Black mafic rock that weathers to light rust color and erodes to a yellow-brown granulated soil. Poor exposure of solid outcrop, but highly jointed where exposed. In thin section, plagioclase shows felty texture and elongate mineral alignment, extensive sericite alteration, and ≤1 mm domains of uralite alteration. Age relationship poorly constrained given lack of contact outcrop, presumed intrusive given the holocrystalline groundmass. *Distinguishing features: microcrystalline black rock that weathers to light rust or yellow. Phenocrysts: 25%, Hbl: 80% (uralite), Oxides: 20%*

PlMlb1 Basalt lava flow (Pliocene to Miocene) A ledge-forming, columnar jointed basalt that is dark gray where fresh and black to dark rust where weathered. Porphyritic with abundant 1 mm plagioclase and orthopyroxene phenocrysts surrounded by black and red banded groundmass and small olivine phenocrysts. Glomerocrysts of plagioclase and pyroxene visible in thin section. Thickness 10–15 m. *Distinguishing features: plagioclase, orthopyroxene, and olivine phenocrysts. Phenocrysts: 40%, Pl: 76%, Ol: 12%, Opx: 12%*

PlMlb2 Aphanitic basalt lava flow (Pliocene to Miocene) Forms an extensive plateau at the southern end of the field area, Table Mountain, and sits unconformably atop the Mesozoic basement rocks. A ledge former with 1 to 2 m hexagonal jointing that lacks consistent orientation. Hand sample is markedly aphanitic with flattened vesicles. Microcrystalline plagioclase visible in thin section. *Distinguishing features: aphanitic black ledge former. Pl: 86% Oxides: 14%*

Miocene Sedimentary Rocks

Mles Esmeralda sands, massive volcanic ash and sands (Miocene) Massive volcanic ash and sands. Forms white ledges with tafoni and smoothly weathered surfaces. Rounded ≤15 cm volcanic clasts suspended in matrix of coarse sands and muds rich in lithics. ~80% matrix, a lithic arkose. Interbedded with crystal-rich, very fine, white ash material. Cuspate glass shards visible in thin section. Thickness ≤100 m. Anorthoclase from volcanic ash yields a $^{40}Ar/^{39}Ar$ age of 11.8 ± 0.1 Ma (this study). *Distinguishing features: coarse sands interbedded with ash.*

Mle Esmeralda Formation, (Miocene) Bedded white silts and muds. Thin (10–15 cm) beds of white and gray silts and muds ranging from silts with highly friable papery texture to densely compacted sands with 3-D current ripples. Near fault contacts beds are strongly deformed. Where beds are intact, sedimentary structures include ripples and flame structures. Papery silt layers composed of stacked ~50 µm diameter Actinocyclus diatoms, suggesting middle Miocene age (Krebs et al., 1987). Thickness of unit in region surrounding map area ~1000 m (Ekren and Byers Jr., 1985a). *Distinguishing features: fine silts, muds, and diatomaceous earth.*

Miocene Basaltic and Andesitic Volcanic Rocks

Mlb Basalt lava flow (Miocene) An olivine-bearing basalt lava. Ledge-forming black basalt that weathers to dark rust color with poorly developed ~1 m wide columns and ~5 cm spaced platy jointing. Subhorizontal veins found at the base of the unit are filled with quartz geodes. Distinguishable from unit Ꞧlg by lack of hornblende. Microcrystalline plagioclase in thin section shows felty texture and 0.5–1.5 mm glomerocrysts of plagioclase and pyroxenes. Groundmass $^{40}Ar/^{39}Ar$ age of 15.71 ± 0.03 Ma (this study). Thickness 5–10 m. *Distinguishing features: olivine phenocrysts. Phenocrysts: 10%, Pl: 50%, Ol: 50%*

Mlal Andesite lava flow (Miocene) A hornblende-bearing andesite lava. Ledge-forming blue-gray or dark gray-black that weathers to a dark rust color. Three distinguishable sections, presumed to be separate flows; base of unit characterized by well-developed columnar jointing and platy jointing; middle of unit is dense, gray, and

foliated; upper section is dark and relatively phenocryst-poor with randomly oriented cooling joints. Conspicuous needle-shaped 1–2 mm hornblende phenocrysts with thick oxide alteration rims to nearly complete oxide replacement. Plagioclase $^{40}Ar/^{39}Ar$ isochron age of 15.99 ± 0.05 Ma (this study). Total thickness where all sections present 70–100 m. *Distinguishing features: hornblende phenocrysts in dark groundmass. Phenocrysts: 47% Pl: 85%, Cpx: 5%, Hbl: 10%*

Mrat Andesite tuff (Miocene) A hornblende-bearing andesite tuff. Slope-forming and poorly exposed lithic-rich tuff with poorly welded white ash matrix. Light-gray to white where fresh, weathers to white granulated soil. Lithic-rich (40%) with local Mesozoic rocks and hornblende-bearing volcanic rocks. Pumice clasts up to 30 cm in diameter with euhedral ≤1.5 mm plagioclase and ≤2 mm hornblendes with oxide alteration rims. Highly variable thickness ≤100 m. *Distinguishing features: lithic-rich tuff with hornblende phenocrysts. Phenocrysts: 37% Pl: 67%, Cpx: 6%, Hbl: 27%, Lithics: 40%, Glassy Mafic: 50%, Mafic Intrusive: 12%, Carbonate: 25%, Felsic Plutonic: 13%*

Other Miocene Sedimentary Rocks

Mrac Alluvium (Miocene) Rounded cobbles of primarily Oligocene volcanic rocks, i.e., the Benton Spring Group. Slopes of unconsolidated well-rounded clasts of gravel to cobbles up to ~20 cm in diameter. Clasts commonly weather to light rust color, yielding a red hued aerial extent in aerial photo. Clast lithologies include granite, limestone, mudstone, vesiculated rhyolite lava, and quartz-rich welded ash. Highly variable thickness ≤100 m. *Distinguishing features: red stained, unconsolidated, rounded cobbles of Benton Spring volcanic rocks.*

Rhyolite Lava Flows

Mrrl Rhyolite of Gabbs Valley Range (Miocene) A flow-laminated biotite rhyolite. White to light-purple rounded cliffs with well-developed foliation. Weakly devitrified glassy groundmass leads to highly friable material that weathers to granular white soil. Conspicuous ≤1 mm biotite flakes in white matrix diagnostic in hand sample. Rounded plagioclase grains ≤3 mm. Extensive ≤1 mm quartz grains with embayment visible in thin section. Plagioclase $^{40}Ar/^{39}Ar$ age of 20.194 ± 0.265 Ma (Dubyoski et al., 2016). Thickness 10–30 m. *Distinguishing features: friable white, rounded cliffs with biotite. Phenocrysts: 45%, Pl: 45, Bt: 22%, Qtz: 22%, Hbl: 11%.*

Mount Ferguson Volcanic and Sedimentary Rocks

Mrlf Lavas of Mount Ferguson, undivided (Miocene) Multiple dense phenocryst-rich flows of varying composition and texture, ranging from light-gray hornblende-rich to dark-red with 3 mm plagioclase phenocrysts. Mostly dark brown and ledge forming, weathers to dark rust or black. Consistently oriented columnar jointing is uncommon, though talus boulders are commonly hexagonally shaped. In phenocryst-rich samples, a clear dark-red and black banding texture is diagnostic throughout the field area. Plagioclase ≤3 mm show spongy-cellular growth and hornblendes ≤1 mm show near complete oxide replacement visible in thin section. K/Ar ages range from 15–22 Ma (Ekren and Byers Jr., 1985a). Plagioclase $^{40}Ar/^{39}Ar$ age of 18.91 ± 0.03 Ma (this study). Thickness 100–200 m. *Distinguishing features: Hornblende and plagioclase phenocrysts in dark brown, commonly banded groundmass. Phenocrysts: 50%, Pl: 60%, Hbl: 10%, Cpx: 30%.*

Mrs Mount Ferguson volcanoclastic rocks (Miocene) Hornblende-bearing tuff and lahar deposits interbedded with tuffaceous fluviolacustrine deposits. Bottom of the unit primarily fine sands and muds interbedded with tuffaceous course grained sands. Moving up section, a slope-forming white and gray, lithic-rich tuff reworked in some places as evidenced by crossbreds in tuffaceous sediments. The tuff is interbedded and overlain by debris flows primarily composed of Mount Ferguson volcanic rocks with boulders ≤1.5 m diameter and petrified logs ≤2 m in length, 0.5 m diameter. Thickness ≤150 m. *Distinguishing features: Petrified wood bearing tuff and mud-flow deposits interbedded with fine sediments.*

Other Miocene Volcanic and Intrusive Rocks

Mrmi Mafic intrusions (Miocene) A dark brown or gray basaltic andesite including phenocrysts of plagioclase and pyroxene (Ekren and Byers Jr., 1985a). Plagioclase $^{40}Ar/^{39}Ar$ age of 23.96 ± 0.23 Ma (Dubyoski et al., 2016). *Distinguishing features: gray basaltic andesite.*

Mrrc Tuff of Redrock Canyon (Miocene) A rhyodacite to quartz latite. Most of the unit is poorly welded, slope-forming gray ash that stains orange-brown. Where moderately welded and ledge-forming there are abundant fiamme ≤10 cm in length and randomly oriented columnar jointing. Lithics of Mesozoic granites and volcanic rocks ≤20 cm in diameter. Phenocryst-rich with ≤2 mm plagioclase and ≤2 mm embayed quartz. Significant prehnite content, likely contributing to yellow outcrop color. Sanidine $^{40}Ar/^{39}Ar$ age of 22.95 ± 0.04 Ma (Lee et al., in review). Thickness ≤150 m. *Distinguishing features: rounded yellow cliffs with pebble-sized lithic fragments. Phenocrysts: 35%, Pl: 57%, Bt: 15%, Qtz: 28%, Hbl: trace, Lithics: 20%.*

Mrlr Hu-pwi Rhyodacite (Miocene) A densely welded, flow-banded rhyodacite tuff. Cliff-forming, black, glass-rich tuff that weathers to light rust color. Very resistant, leaving sharp joint intersections on cliff faces. Fractures colloidally into sharp glassy shards. Vitrified, flattened fiamme ≤10 cm long create tiger-stripe texture at outcrop scale. Plagioclase phenocrysts and lithics clearly visible in hand sample.

Plagioclase has spongy cellular texture and rounded grain boundaries. Thickness 10–30 m. *Distinguishing features: densely welded tuff with glassy bands of 10 cm long fiamme. Phenocrysts: 45%, Pl: 77%, Hbl: 6%, Cpx: 17%, Lithics: 10%.*

Oligocene Tuffs

Ogln Lavas of Nugent Wash (Oligocene) A hornblende-bearing andesite lava. Slope forming dark red-brown to dark gray. Flow banding layers ≤8 mm thick with plagioclase and hornblende phenocrysts 1–10 mm (Mayberry and Lee, 2017). Thickness ≤200 m. *Distinguishing features: layers of ≤10 mm phenocrysts.*

Ogsp Blue Sphinx Tuff (Oligocene) A quartz latite. Light gray moderately welded ledge-former that easily weathers to red-gray rounded face. Light purple or white on fresh face. Diagnostic white pumice up to 3 cm and conspicuous ≤1.5 mm embayed quartz surrounded by biotite-rich, purple groundmass visible in hand sample. Poorly developed flow foliation. In thin section, 2 mm plagioclase phenocrysts are highly irregular with abundance of small (50 µm) fragments. Significant prehnite growth in void space suggesting hydrothermal alteration. Sanidine $^{40}Ar/^{39}Ar$ age of 24.30 ± 0.05 Ma (Henry and John, 2013). Thickness ≤30 m. *Distinguishing features: white to purple rounded cliffs rich in embayed quartz. Phenocrysts: 40%, Pl: 40%, Hbl: 14%, Qtz: 40%, Bt: 6%.*

Benton Spring Group

Ogbp Petrified Spring Tuff of Benton Spring Group (Oligocene) A biotite and plagioclase-bearing poorly welded tuff. Dark gray-brown poorly welded tuff rich in lithic fragments giving it a conglomerate-like appearance at outcrop scale. Weathers to rounded ledges with meter-scale tafoni. Diagnostic 40 cm flattened, white pumice clasts easily recognizable against gray matrix. Friable material consisting ~30% of angular lithics ~2 cm in diameter and dark gray, biotite-rich ash matrix. Flattened cuspate shaped glass fragments visible in thin section. Thickness ≤100 m. *Distinguishing features: rounded gray cliffs with ≤40 cm white fiamme. Phenocrysts: 15%, Pl: 67%, Bt: 33%, Lithics: 30%*

Ogbsi Singatse Tuff of Benton Spring Group (Oligocene) A rhyodacite to rhyolite tuff. Multiple cooling units of varying degrees of welding, generally slope-forming. Most easily distinguishable by the dark red color and presence of granitic lithics. Flaggy outcrop pattern that weathers to rust color. ≤2.5 mm Plagioclase, quartz, and ≤1 mm biotite clearly visible in hand sample. Densely welded in southern section of field area with clear flow banding textured brown-red glass and well-developed hexagonal joints. Sanidine $^{40}Ar/^{39}Ar$ age of 26.85 ± 0.02 Ma (Henry and John, 2013). Thickness ≤300 m. *Distinguishing features: red and gray banded tuff with lithics, quartz, and biotite. Phenocrysts: 40%, Pl: 37%, Bt: 7%, Or: 25%, Hbl: 5%, Qtz: 25%, Lithics: 15%*

Ogbmg Guild Mine Member of Mickey Pass Tuff of Benton Spring Group (Oligocene) A rhyodacite to rhyolite tuff. Multiple cooling units with variable color and composition. Basal flow-banded vitrophyre characterized by abundant gray lithics (≤30%) and purple-dark gray flow banding. Weathers to dark brown with weathered out fiamme pits ≤5 cm in length. Up section lithics are rare and quartz phenocrysts abundant. Upper section forms white flaggy outcrop pattern that weathers to rusty yellow. Lack of large fiamme make foliation orientations difficult to observe. ≤2 mm Quartz and biotite phenocrysts are found throughout and are diagnostic for unit. Embayment of quartz phenocrysts visible in thin section. Sanidine $^{40}Ar/^{39}Ar$ age of 27.24 ± 0.04 Ma (Henry and John, 2013). Thickness ≤300 m. *Distinguishing features: purple and gray banded tuff with quartz, and biotite; lithics in basal section. Phenocrysts: 40%, Or: 50%, Qtz: 45%, Bt: 5%*

Oligocene Lava Flows

Ogalg Lavas of Giroux Valley (Oligocene) A pyroxene-bearing phyric basalt lava. Ledge-forming dense black basalt that weathers to angular gravel talus. Very dark and dull on fresh surface that weathers to dark rust color. Upper section forms regularly oriented columnar joints with ≤1.5 mm hornblende phenocrysts. Hornblende and ≤2 mm pyroxene phenocrysts and glomerocrysts of pyroxenes and plagioclase with spongy-cellular growth textures. *Distinguishing features: dull black columns that weather to dark rust color. Phenocrysts: 55%, Pl: 45%, Cpx: 27%, Hbl: 18%, Ol: 10%*

Mesozoic Rocks

KJqm Quartz monzonite (Cretaceous to Jurassic) Gray to green rounded cliffs generally found cresting the highest ridges in the field area. Where freshly exposed parallel jointing is common, also found as rounded corestones in paleosols. Medium grained phaneritic with abundant quartz veins. *Distinguishing features: rounded white cliffs with spheroidal boulders. Pl: 40%, Bt: 10%, Or: 25%, Hbl: 5%, Qtz: 15%, Ttn: 5%*

Jdi Diorite (Jurassic) Dark green cliffs with parallel jointing. Phaneritic and weathers to dark brown (Ekren and Byers, 1985a). *Distinguishing features: dark green jointed cliffs.*

Jd Dunlap Formation (Jurassic) Red cross-bedded sands interbedded with shale. Shale interbedded with sands and conglomerates containing clasts of limestone and chert (Ekren and Byers Jr., 1985a). *Distinguishing features: red cross-bedded sands and shales.*

TRlu Luning Formation (Triassic) Undivided dolomites, limestones, and shales. Blue and gray rounded cliffs of highly deformed carbonate rocks ranging in composition and texture. Skarn deposits regularly found at contact with Mesozoic intrusive rocks. *Distinguishing features: blue and gray cliffs of limestones and dolomites.*

ACKNOWLEDGMENTS

Thanks to Drew Abts for his exceptional field assistance. Field discussions with Joe Colgan, Chris Henry, David John, and Sarah Nagorsen were invaluable. We thank Dean Miller, James Saburomaru, and Katie Sullivan at the USGS in Menlo Park for help with sample separation and irradiation preparations. Funding for this project was provided by National Science Foundation grant EAR-1419808, and a U.S. Geological Survey National Cooperative Geologic Mapping Program grant G17AC00197, awarded to J. Lee. Additional funding was provided by a Geological Society of America graduate student research grant, 11768-17, awarded to A. Hoxey, and the Geological Society of Nevada. Stereonet plots were produced using Stereonet 9.9.3 software thanks to Rick Allmendinger. Thanks to Seth Dee, Rachel Micander, and Jennifer Vlcan for their careful and thorough editing of the geologic map, cross sections, and text.

The views and conclusions contained in this document are those of the authors and should not be interpreted as necessarily representing the official policies, either expressed or implied, of the U.S. Government.

REFERENCES

Bennett, R.A., Wernicke, B.P., Niemi, N.A., Friedrich, A.M., and Davis, J.L., 2003, Contemporary strain rates in the northern Basin and Range Province from GPS data: Tectonics, v. 22, doi: 10.1029/2001TC001355.

Bormann, J.M., Hammond, W.C., Kreemer, C., and Blewitt, G., 2016, Accommodation of missing shear strain in the central Walker Lane, western North America—constraints from dense GPS measurements: Earth and Planetary Science Letters, v. 440, p. 169–177, doi: 10.1016/j.epsl.2016.01.015.

Colgan, J.P., and Henry, C.D., 2017, Eruptive history, geochronology, and post-eruption structural evolution of the late Eocene Hall Creek caldera, Toiyabe Range, Nevada: doi: 10.3133/pp1832.

Dalrymple, G.B., and Duffield, W.A., 1988, High precision $^{40}Ar/^{39}Ar$ dating of Oligocene rhyolites from the Mogollon-Datil volcanic field using a continuous laser system: Geophysical Research Letters, v. 15, p. 463–466, doi: 10.1029/GL015i005p00463.

Dilles, J.H, and Gans, P.B. 1995, The chronology of Cenozoic volcanism and deformation in the Yerington area, western Basin and Range and Walker Lane: GSA Bulletin, v. 107, p. 474–486, doi: https://doi.org/10.1130/0016-7606(1995)107<0474:TCOCVA>2.3.CO;2.

Dixon, T.H., Robaudo, S., Lee, J., and Reheis, M.C., 1995, Constraints on present-day Basin and Range deformation from space geodesy: Tectonics, v. 14, p. 755–772, doi: 10.1029/95TC00931.

Dokka, R.K., and Travis, C.J., 1990, Role of the eastern California shear zone in accommodating Pacific–North American plate motion: Geophysical Research Letters, v. 17, doi: 10.1029/GL017i009p01323.

Dubyoski, P., Calvert, A.T., and Lee, J., 2016, Tuff-filled paleovalleys dextrally offset across the Benton Springs fault, central Walker Lane, Nevada, *in* Geological Society of America Abstracts with Programs, Denver, CO, v. 48, p. 267–18, doi: 10.1130/abs/2016AM-283180.

Ekren, E.B., and Byers Jr., F.M., 1985a, Geologic map of the Gabbs Mountain, Mount Ferguson, Luning, and Sunrise Flat quadrangles, Mineral and Nye counties, Nevada: http://pubs.er.usgs.gov/publication/i1577.

Ekren, E.B., and Byers Jr., F.M., 1986a, Geologic map of the Mount Annie NE, Mount Annie, Ramsey Spring, and Mount Annie SE quadrangles, Mineral and Nye counties, Nevada: http://pubs.er.usgs.gov/publication/i1579.

Ekren, E.B., and Byers Jr., F.M., 1986b, Geologic map of the Murphys Well, Pilot Cone, Copper Mountain, and Poinsettia Spring quadrangles, Mineral County, Nevada: http://pubs.er.usgs.gov/publication/i1576.

Ekren, E.B., and Byers Jr., F.M., 1985b, Geologic map of the Win Wan Flat, Kinkaid NW, Kinkaid, and Indian Head Peak quadrangles, Mineral County, Nevada: http://pubs.er.usgs.gov/publication/i1578.

Ekren, E.B., Byers Jr., F.M., Hardyman, R.F., Marvin, R.F., and Silberman, M.L., 1980, Stratigraphy, preliminary petrology, and some structural features of Tertiary volcanic rocks in the Gabbs Valley and Gillis ranges, Mineral County, Nevada: U.S. Geological Survey, Bulletin, p. 54.

Faulds, J.E., and Henry, C.D., 2008, Tectonic influences on the spatial and temporal evolution of the Walker Lane—an incipient transform fault along the evolving Pacific–North American plate boundary *in* Ores and Orogenesis—circum-Pacific tectonics, geologic evolution, and ore deposits: Arizona Geological Society Digest, v. 22, p. 437–470.

Hardyman, R.F., 1980, Geologic map of the Gillis Canyon quadrangle, Mineral County, Nevada: U.S. Geological Survey Miscellaneous Investigations Series Map I-1237, scale 1:48,000.

Henry, C.D., and Faulds, J.E., 2010, Ash-flow tuffs in the Nine Hill, Nevada, paleovalley and implications for tectonism and volcanism of the western Great Basin, USA: Geosphere, v. 6, p. 339–369, doi: 10.1130/GES00548.1.

Henry, C.D., and John, D.A., 2013, Magmatism, ash-flow tuffs, and calderas of the ignimbrite flareup in the western Nevada volcanic field, Great Basin, USA: Geosphere, v. 9, p. 951–1008, doi: 10.1130/GES00867.1.

Krebs, W.N., Bradbury, J.P., and Theriot, E., 1987, Neogene and Quaternary lacustrine diatom biochronology, western USA: PALAIOS, v. 2, p. 505–513, doi: 10.2307/3514621.

Lee, J., Hoxey, A.R., Calvert, A., and Dubyoski, P., in review, Plate boundary trench retreat and dextral shear drive intracontinental fault slip histories—Neogene faulting across the Gabbs Valley and Gillis ranges, central Walker Lane, Nevada, submitted 02/04/20 to Geosphere.

Lee, J., Rubin, C.M., and Calvert, A., 2001, Quaternary faulting history along the Deep Springs fault, California: GSA Bulletin, v. 113, p. 855–869, doi: 10.1130/0016-7606(2001)113<0855:QFHATD>2.0.CO;2.

Mayberry, C., and Lee, J., 2017, Tuff-filled paleovalleys dextrally offset by the Gumdrop Hills fault, central Walker Lane, Nevada, *in* Geological Society of America Abstracts with Programs, Seattle, Washington, v. 49, p. Abstract 385-19, doi: 10.1130/abs/2017AM-308732.

Nagorsen-Rinke, S., Lee, J., and Calvert, A., 2013, Pliocene sinistral slip across the Adobe Hills, eastern California-western Nevada—kinematics of fault slip transfer across the Mina deflection: Geosphere, v. 9, p. 37–53, doi: 10.1130/GES00825.1.

Oldow, J.S., and Dockery, H.A., 1993, Geologic map of the Mina quadrangle, Nevada: Nevada Bureau of Mines and Geology Field Studies Map 6, scale 1:24,000.

Oldow, J.S., and Meinwald, J.N., 1992, Geologic map of the Bettles Well quadrangle, Nevada: Nevada Bureau of Mines and Geology Field Studies Map 1, scale 1:24,000.

Stockli, D.F., Dumitru, T.A., McWilliams, M.O., and Farley, K.A., 2003, Cenozoic tectonic evolution of the White Mountains, California and Nevada: GSA Bulletin, v. 115, p. 788–816, doi: 10.1130/0016-7606(2003)115<0788:CTEOTW>2.0.CO;2.

Wesnousky, S.G., 2005, Active faulting in the Walker Lane: Tectonics, v. 24, p. 1–35, doi: 10.1029/2004TC001645.

Wright, H.M.N., Lesti, C., Cas, R.A.F., Porreca, M., Viramonte, J.G., Folkes, C.B., and Giordano, G., 2011, Columnar jointing in vapor-phase-altered, non-welded Cerro Galán Ignimbrite, Paycuqui, Argentina: Bulletin of Volcanology, v. 73, p. 1567–1582, doi: 10.1007/s00445-011-0524-6.

Suggested Citation:

Hoxey, A., Lee, J., and Calvert, A., 2020, Geologic map of the Petrified Spring fault, Gabbs Valley Range, Mineral County, Nevada: Nevada Bureau of Mines and Geology Open-File Report 20-1, 2 sheets, scale 1:24,000, 14 p.

© Copyright 2020 The University of Nevada, Reno. All Rights Reserved.